Crystallinity in liquid films

Hartmut Löwen and Thomas Beier
Sektion Physik der Universität München, Theresienstrasse 37, D-8000 München 2, Federal Republic of Germany
(Received 7 June 1989; revised manuscript received 8 August 1989)

If a solid is covered with a quasi-liquid-film, each Fourier coefficient of the solid density vanishes with a characteristic decay length within the liquid film. A microscopic theory is employed in order to calculate these decay lengths and to study their dependence on the orientation of the surface plane and on the microscopic interaction potential. The results are compared with recent surface experiments on Pb.

I. INTRODUCTION

Consider a planar solid-liquid interface and let $\mathbf{G}$ denote a reciprocal-lattice vector (RLV) of the bulk crystal. As one moves through the interface, the local mean density ρ_0 changes from the solid mean density to the liquid density. Simultaneously, each Fourier coefficient $\rho_{\mathbf{G}}$ ($\mathbf{G}\neq\mathbf{0}$) of the solid density decays to zero in the liquid with a characteristic decay length $a_{\mathbf{G}}$.

The decay lengths are accessible experimentally by surface scattering experiments. In particular, one may examine quasi-liquid-films on a solid and measure the residual crystallinity in the quasi-liquid-gas interface. The thickness of the quasi-liquid-film increases with temperature. Recently, the structure of the Pb(110) interface was studied by Prince and co-workers[1,2] using low-energy electron diffraction (LEED). They found that the decay length of a density oscillation with RLV $\mathbf{G}$ decreases if the projection of $\mathbf{G}$ onto the surface plane increases.

In order to explain these findings, Lipowsky *et al.*[3] have used a phenomenological square-gradient Landau theory, where a multicomponent order parameter (OP) is introduced. Each OP component is the amplitude of a density oscillation with a RLV $\mathbf{G}^{\parallel}$ of the two-dimensional lattice planes parallel to the surface. However, in comparison with experiment, the Landau theory yields decay lengths that are too small by a factor of $\cong\frac{1}{3}$.

In this paper, we extend this Landau theory in several directions: (i) We employ a more detailed model, where each OP component is the amplitude of a density oscillation with a RLV of the *full* bulk crystal lattice. (ii) We include OP gradients to arbitrary order. (iii) We calculate the decay length of each OP component within a microscopic theory.

As a result, we confirm that the decay lengths decrease with increasing $|G^{\parallel}|$. However, the microscopically calculated decay lengths are larger than predicted by the Landau theory of Ref. 3 and closer to the experimental data.

We proceed as follows: In Sec. II, a microscopic expression for the decay lengths of the different Fourier components of the solid density is derived. This involves the Fourier transform of the Ornstein-Zernike correlation function $c(k)$ of the bulk liquid phase. Then, in Sec. III, we calculate the decay lengths for a simple model potential and examine the influence of an oscillating tail in the pairwise forces. In Sec. IV, we use experimental data of the liquid structure factor to deduce the decay lengths in liquid Pb and Al. Finally, in Sec. V, the influence of higher-order corrections and long-ranged potentials is discussed.

II. MICROSCOPIC THEORY

In order to describe a solid-liquid interface, we parametrize the local density by

$$\rho(\mathbf{r})=\sum_{\mathbf{G}}\rho_{\mathbf{G}}(z)\exp(i\mathbf{G}\cdot\mathbf{r}),\quad \rho_{\mathbf{G}}^{*}(z)=\rho_{-\mathbf{G}}(z)\ . \tag{1}$$

The complex Fourier coefficients $\rho_{\mathbf{G}}$ are taken as order parameters, which vary in the z direction perpendicular to the surface plane and fulfill the boundary conditions

$$\rho_{\mathbf{G}}(z\rightarrow-\infty)=\rho_{\mathbf{G}s},\quad \rho_{\mathbf{G}}(z\rightarrow\infty)=\delta_{\mathbf{G},\mathbf{0}}\rho_l\ , \tag{2}$$

where $\rho_{\mathbf{G}s}$ are the solid bulk values and ρ_l the liquid density. Now a gradient expansion[4] of the density functional around the liquid phase yields the asymptotic form of $\rho_{\mathbf{G}}(z)$ for $z\rightarrow\infty$. This is described in more detail by Mikheev and Chernov.[5] For the moment, we consider only terms bilinear in the OP's and assume short-ranged particle interactions. The influence of higher-order corrections and long-ranged potentials is discussed in Sec. V. Within the gradient expansion, we arrive at the asymptotic result for $z\rightarrow\infty$,

$$\rho_{\mathbf{G}}(z)-\delta_{\mathbf{G},\mathbf{0}}\rho_l\sim\exp(ik_{\mathbf{G}}z)\exp(-z/a_{\mathbf{G}})\ . \tag{3}$$

Here, $k_{\mathbf{G}}$ is a phase mismatch between the solid and liquid density: In the liquid, the most probable position of a next-neighbor particle differs slightly from the solid nearest-neighbor spacing, which results in an additional small oscillation in the OP's. Furthermore, $a_{\mathbf{G}}$ is the decay length of $\rho_{\mathbf{G}}$ within the liquid. The asymptotic analysis[5] shows that $k_{\mathbf{G}}$ and $a_{\mathbf{G}}$ are given by complex zeroes of the second direct correlation function of the liquid in Fourier space, denoted by $c(k)$. More specifically, consider the complex solutions k of

$$c([G^{\parallel 2}+(G^{\perp}-k)^2]^{1/2})-1/\rho_l=0\ , \tag{4}$$

where $\mathbf{G}=(\mathbf{G}^{\parallel},G^{\perp})$, written in components parallel and perpendicular to the surface plane. Then, $1/a_{\mathbf{G}}=\min(\mathrm{Im}(k))$. Here the minimum is over all solutions of (3), where $k_{\mathbf{G}}=\mathrm{Re}(k)$ lies in the projection of the first Brillouin zone (1PBZ) of the solid lattice on the z axis.

This can be rewritten as follows. Let $\{q_j=u_j+iv_j\}$ be the set of all complex solutions of

$$c(q_j)-1/\rho_l=0 \ . \tag{5}$$

This equation is also known from the theory of spinodal decomposition. q is the complex wave number of a density perturbation in the liquid phase. With the abbreviation

$$w_j\equiv(u_j^2-v_j^2-G^{\parallel 2})/2 \ ,$$

we obtain

$$a_{\mathbf{G}}^{-2}=\min_j(w_j+(w_j^2+u_j^2v_j^2)^{1/2}) \ . \tag{6}$$

As already stated earlier, the minimum extends over all solutions q_j whose wave vector

$$u_jv_j(w_j+(w_j^2+u_j^2v_j^2)^{1/2})+G^{\perp}$$

lies in 1PBZ. Without loss of generality, let the right-hand side of (6) be minimal for $j=0$. Then

$$k_{\mathbf{G}}=u_0v_0a_{\mathbf{G}}+G^{\perp} \ . \tag{7}$$

Equations (6) and (7) are the central result of this section.

Thus the problem is reduced to find the complex solutions q_j of (5). This can be done in two ways. First, one can use experimental data of the liquid structure factor $S(k)$. Then, in a quadratic approximation[6]:

$$u_j=q_{mj} \ . \tag{8}$$

Here, q_{mj} is a real wave number, where $S(k)$ has a local maximum. Moreover,

$$v_j=\{2/[S(q_{mj})L''(q_{mj})]\}^{1/2} \ , \tag{9}$$

with $L(k)\equiv 1/S(k)$, primes denoting derivatives with respect to k. We will use Eqs. (8) and (9) in Sec. IV.

Second, one can calculate $\{q_j\}$ within a microscopic theory with the interparticle potential $\phi(r)$ as the only input, see the following section.

Once the $a_{\mathbf{G}}$'s are known, the residual crystallinity at the quasi-liquid-gas interface can be calculated. As a function of the reduced temperature $t=(T_T-T)/T_T$, where T_T denotes the triple temperature, the residual crystallinity for a density oscillation with RLV $\mathbf{G}$ vanishes as a power law with exponent[4]

$$\nu_{\mathbf{G}}=\max(2a_0,\{a_{\mathbf{G}}\})/(2a_{\mathbf{G}}) \ . \tag{10}$$

III. CALCULATION OF DECAY LENGTHS FOR A SIMPLE MODEL POTENTIAL

In this section, we calculate $a_{\mathbf{G}}$ and $k_{\mathbf{G}}$ for a simple model potential $\phi(r)$: we take a hard core with diameter σ and an attractive Lennard-Jones-type potential $\phi_a(r)$ as an example (see inset of Fig. 1)

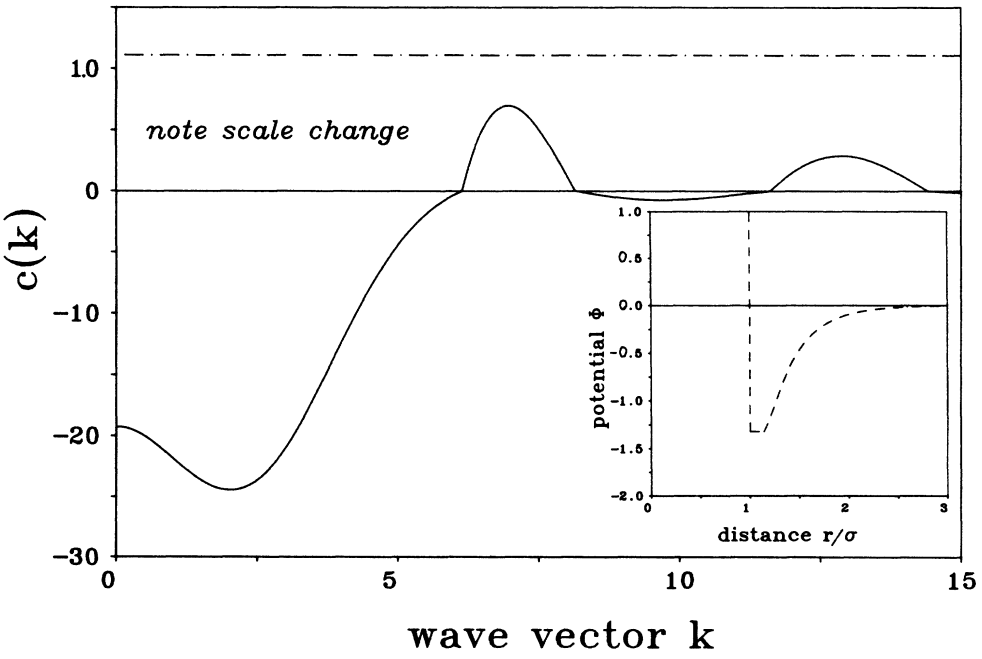

FIG. 1. Fourier transform of the direct correlation function in units σ^3 (solid line). Note the scale change. The wave vectors are in units $1/\sigma$. The dotted-dashed line is the constant $1/\rho_l$. The inset shows the associated hard sphere plus Lennard-Jones potential in units k_BT. The parameters are as in Table I.

$$\phi_a(r)=\begin{cases} w(r)\equiv E\{\exp[-a(x-1)]-\exp[-b(x-1)]\}/x, & x=r/\sigma \text{ for } r>d, \\ w(d) \text{ for } \sigma\le r\le d, \end{cases} \tag{11}$$

where we choose $d=1.1414\sigma$ and take the parameters $E=2.0199\varepsilon$, $a=14.735$, $b=2.6793$ from the Foiles-Ashcroft parametrization[7] of a Lennard-Jones potential. Model potentials of this kind are familiar in the theory of liquids, see Ref. 8.

There are several approximations to obtain $c(k)$ from $\phi(r)$ (see, e.g., Refs. 8 and 9), the crudest one is the high-temperature approximation (HTA), which approximates the true $c(k)$ by the direct correlation function of hard cores. For the latter the Percus-Yevick expression [denoted by $c_{\rm PY}(k)$] or the more accurate Verlet-Weis form [denoted by $c_{\rm VW}(k)$] (Ref. 10) can be used. The HTA clearly neglects effects of an attractive tail. To include such a tail more accurately, we use the optimized random-phase approximation (ORPA),

$$c(k)=c_{\rm VW}(k)-\tilde{\phi}_a(k)/(k_BT)+\tilde{\Delta}(k)\ , \tag{12}$$

with $\Delta(r)=0$ for $r>\sigma$, $\tilde{\phi}_a(k)$, and $\tilde{\Delta}(k)$ denoting the Fourier transforms of $\phi_a(r)$ and $\Delta(r)$, respectively. Here, $\Delta(r)$ is determined by the condition that the pair correlation $g(r)$ vanishes for $r<\sigma$. The pair correlation $g(r)$, in turn, is linked with $c(k)$ via the Ornstein-Zernike relation. We approximate $\Delta(r)$ by a polynomial to second order in r for $r<\sigma$ and optimize its coefficients. For a situation near the triple point, the resulting $c(k)$ is shown for real k in Fig. 1.

The intersection points of $c(k)$ with $1/\rho_l$ for complex k will be near the local maxima of $c(k)$ for real k, see Fig. 1. The results for this solutions q_j are summarized in Table I. For comparison, also the HTA results are given. Remarkably, they do not possess a solution with $u_j=0$. This corresponds to the fact that $c(k)$ has a minimum for $k=0$. The quadratic approximation around the local maxima of $c(k)$ for real k is only slightly in error of 10–15 %, in general. However, for $u=0$ it is wrong by a factor of 3; therefore quartic corrections are necessary to find the zero of (5) with $u=0$.

Using Eqs. (6) and (7) we display the mismatch and the correlation length for different RLV of an fcc lattice in Fig. 2 for a (111) plane. This clearly shows that the smectic order (represented by $a_{(111)}$) decays much slower than the parallel order. Furthermore, higher Fourier coefficients have a smaller decay length. As for the exponent of the residual crystallinity [see (10)] we find $\nu_{(111)}=0.5$ and $\nu_{(-111)}=1.3$. This can be compared with the numerical result of Trayanov and Tosatti[11] who only considered one single crystal OP and found $\nu=1.6$. However, one should note that ν depends sensitively on the cutoff in the Lennard-Jones potential.

For a (100) plane, $a_{(111)}$ is reduced since its RLV is no longer parallel to the surface normal; in this case we have $a_{(111)}<2a_{(000)}$. Physically more interesting is the (110) plane, where melting was observed experimentally. We shall discuss this orientation in the next section.

Next, we consider an oscillatory short-ranged potential by adding

$$\phi_{\rm osc}(r)=A\Theta(9\sigma-r)\exp(-\beta r)\sin(k_Fr)/r$$

to (11), where Θ denotes the step function and k_F is the Fermi momentum. Potentials of this kind have been employed to describe liquid metals.[12,13] Using $1/\beta=7\sigma$, $k_F\sigma=6.88$, $A\sigma=-0.25k_BT/\pi$, and the parameters of Fig. 1 we obtain within the ORPA that the correlation lengths of the crystal OP's are enhanced considerably. For the same parameters as in Fig. 2 we find $u=7.31$, $v=0.32$. This corresponds to $a_{(111)}=3.2\sigma$ for a (111) plane of an fcc solid.

If $\phi_a(k)$ has a minimum where the hard-sphere $c(k)$ has a maximum, then the total $c(k)$ will have a higher and sharper maximum, which leads to an enhancement of the correlation length due to a resonance between the potential and density oscillations. Since $k\cong k_F\cong|G_1|$, this is the case in the example studied before. On the other hand, if $\phi_a(k)$ has a maximum where $c(k)$ has a maximum, the correlation length will decrease. However, this simple picture is modified by the ORPA procedure. So we even find in the preceding case, that $a_{(000)}$ and $a_{(222)}$ were enhanced, too, such that $\nu_{\rm G}$ and other ratios of decay lengths do not vary drastically.

Up to now, we have studied hard cores. The numerical values for $a_{\rm G}$ may also vary for a soft core, but this should not be a big effect.

Summarizing, we have established a connection between the decay lengths $a_{\rm G}$ of the crystallinity within the liquid film and the direct correlation function $c(k)$ of the liquid. In general, $c(k)$ depends on the interparticle potential and, on the one hand, the decay lengths are nonuniversal. On the other hand, physically reasonable liquid structure factors can often be well parametrized by the structure factor of a hard-sphere liquid with suitably

TABLE I. Complex solutions of (5), $q_j=u_j+iv_j$ in units of $1/\sigma$ for a hard sphere plus Lennard-Jones potential for a situation near the triple point ($\rho_l=0.9\sigma^{-3}$, $k_BT/\varepsilon=0.75$). Both the ORPA and, for comparison, HTA results are given. For the latter the Verlet-Weis (VW) and the less accurate Percus-Yevick (PY) approximations are shown.

	ORPA	HTA-PY	HTA-VW
u_1+iv_1	$0.00+i1.74$	no solution	no solution
u_2+iv_2	$6.88+i0.69$	$6.82+i0.65$	$6.82+i0.71$
u_3+iv_3	$12.69+i1.88$	$12.60+i1.82$	$12.69+i1.92$

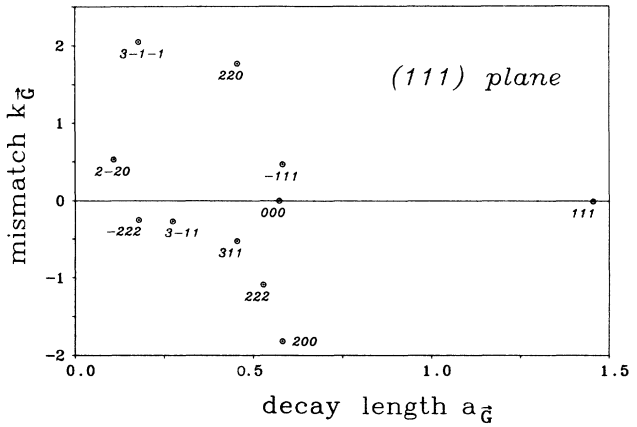

FIG. 2. Mismatch k_G and correlation length a_G (in units of σ^{-1} and σ, respectively) for different reciprocal lattice vectors $\mathbf{G}$. We have chosen an fcc lattice with first RLV $|\mathbf{G}_1|=6.89/\sigma$. The inter-particle potential and further parameters are as in Table I. The surface orientation is a (111) plane. To each point one typical RLV is shown in units of $|\mathbf{G}_1|/\sqrt{3}$.

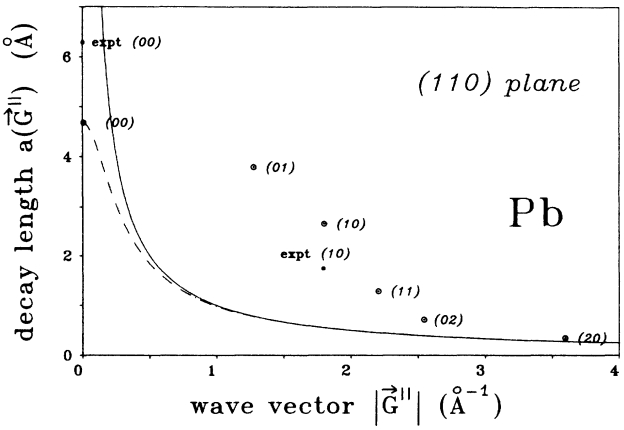

FIG. 3. Decay lengths $a(\mathbf{G}^{\parallel})$, plotted versus $|\mathbf{G}^{\parallel}|$ ($\odot$) for lead at the melting point ($T=600.7$ K). Units are in Å^{-1} and Å. We choose a (110) plane. Each point is labeled by the pair of integers (nm) resulting from $\mathbf{G}^{\parallel}=n\mathbf{G}_1^{\parallel}+m\mathbf{G}_2^{\parallel}$ with $\mathbf{G}_1^{\parallel}\sim(1,-1,0)$, $\mathbf{G}_2^{\parallel}\sim(0,0,1)$. For the (00) and (10) beam, the experimental values are also indicated ($*$). For comparison, the relation (14) is shown (dotted-dashed line), which, for any choice of $a(\mathbf{0})$, is bounded by $1/|\mathbf{G}^{\parallel}|$ (solid line).

chosen diameter. According to the Hansen-Verlet rule,[14] the liquid freezes if the first peak of the liquid structure factor exceeds 2.85. Thus for this class of materials, the ratios $a_G/a_{G'}$, are relatively model independent, for $\mathbf{G},\mathbf{G}'\neq\mathbf{0}$, if the surface orientation is fixed.

IV. RESULTS FOR Pb AND Al

In usual surface scattering experiments decay lengths with same $\mathbf{G}^{\parallel}$ but different $G^{\perp}$ cannot be distinguished. Therefore it is natural to define a decay length $a(\mathbf{G}^{\parallel})$ that only depends on $\mathbf{G}^{\parallel}$ by

$$a(\mathbf{G}^{\parallel})=\max_{G^{\perp}}(a_{(\mathbf{G}^{\parallel},G^{\perp})}) . \tag{13}$$

For these quantities, the Landau theory of Ref. 3 yields the simple algebraic relation

$$a(\mathbf{G}^{\parallel})=a(\mathbf{0})/\{1+[\mathbf{G}^{\parallel}a(\mathbf{G}^{\parallel})]^2\}^{1/2} . \tag{14}$$

It is tempting to compare our result with (14) and with experimental values of $a(\mathbf{G}^{\parallel})$. To achieve this, we first calculate $a(\mathbf{G}^{\parallel})$ within our theory for Pb and Al.

We use experimental data of the liquid structure factor of Pb and Al near the triple point; for a compilation of the data see Waseda.[15] Unfortunately, the data for the liquid structure factor $S(k)$ are not given for the melting temperature T_m of Pb (600.7 K) and Al (931.7 K), but for three temperatures above T_m. We therefore extrapolate $S(k)$ from these values to T_m. Furthermore, we take 18 values near a minimum of $1/S(k)$ and determine an interpolating polynomial of sixth order for $1/S(k)$ by a least-square fit, whose complex zeroes are to be found. The complex solutions $q_j=u_j+iv_j$ of (5) are then in units of Å^{-1}

$$\text{for Pb: } 2.15+i0.213 \quad 4.12+i0.620 , \tag{15}$$

$$\text{for Al: } 2.81+i0.365 \quad 4.80+i0.579 . \tag{16}$$

The resulting $a(\mathbf{G}^{\parallel})$'s are shown in Figs. 3 and 4. It turns out that the expression (14) of the Landau theory underestimates $a(\mathbf{G}^{\parallel})$ considerably.[16] Experimental results are still sparse, the only data we are aware of are from the LEED experiment of Breuer *et al.*,[2] who get for the (10) beam: $a(\mathbf{G}^{\parallel})=1.75$ Å and from ion-scattering experiments of Pluis *et al.*,[17] who obtained $a(\mathbf{0})=6.3$ Å. These data have to be compared with our theoretical values of 2.66 Å and, respectively, 4.7 Å.

The agreement is reasonable, the discrepancies of $\cong -34\%$ and, respectively, $\cong +34\%$ may have several reasons. First, we have not used data of $S(k)$ at the melting point, but extrapolated them from higher temperatures. The first peak of the extrapolated $S(k)$ for T_m is at $\cong 2.5$, which is slower than 2.85 according to the Hansen-Verlet rule.[14] If the first peak would be really higher than 2.5, then the decay lengths a_G would increase. This would make the comparison with the LEED experiment worse, but it improves the comparison with the $a(\mathbf{0})$ data of Ref. 17.

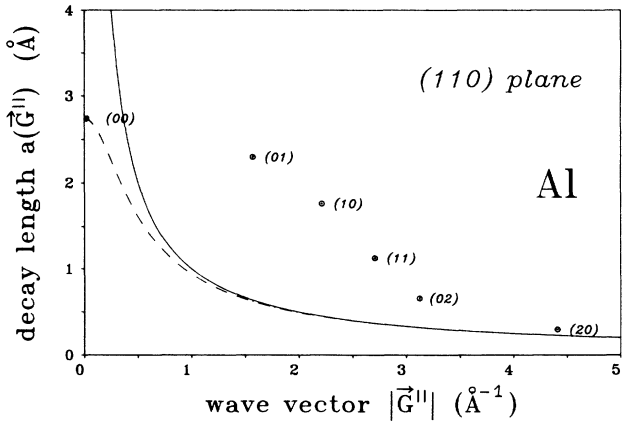

FIG. 4. Same as Fig. 3, but now for Al ($T=931.7$ K). Units are in Å^{-1} and Å.

Second, the discrepancies may result from the experimental side. In Ref. 2, one is still away from the triple point. Furthermore, $a(\mathbf{G}^{\parallel})$ is not measured directly such that one needs a model that expresses the scattering intensity as a function of $a(\mathbf{G}^{\parallel})$. Experimental uncertainties are less pronounced in the ion-scattering experiments,[17] since here $a(\mathbf{0})$ is directly measured as the prefactor of the logarithmic divergence law for the thickness of the quasiliquid layer.

We add as a comment that Landau theory[3] [see (14)] yields for the (01) beam $a((01))\cong 0.56$ Å, which is too small. Moreover, it cannot make any prediction for $a(\mathbf{0})$.

Totally reflected x-ray scattering experiments would be more suitable to determine $a(\mathbf{G}^{\parallel})$ for different $\mathbf{G}^{\parallel}$'s. Such experiments are highly desirable in order to improve the experimental data and to compare with the prediction of other decay lengths than that of the (10) beam.

We add a final remark concerning $a(\mathbf{0})$. In Figs. 3 and 4, $a(\mathbf{0})$ results from a smectic density oscillation with wave vector $\mathrm{Re}(q_1)=u_1$. For a (110) plane, the prefactor of such a density perturbation should be small, since it is incommensurable with the natural lattice spacing. Another example of a density perturbation with $\mathbf{G}^{\parallel}=\mathbf{0}$ is where $G^{\perp}=0$, too. Unfortunately, the experimental data of the liquid structure factor $S(k)$ are not known exactly for $k\cong 0$. Therefore we cannot determine $a_{(000)}$ and $a(\mathbf{G}^{\parallel})$ exactly. We conjecture that in the interesting region $a_{(000)}<a(\mathbf{0})$.

V. INFLUENCE OF HIGHER-ORDER GRADIENTS AND OF LONG-RANGED POTENTIALS

We finally discuss the influence of higher-order terms in the gradient expansion and the effect of long-ranged potentials.

Concerning higher-order corrections, an asymptotic analysis yields the inequality

$$1/a_{\mathbf{G}} \le \sum_{i=1}^{n} 1/a_{\mathbf{G}_i} , \tag{17}$$

provided the sum rule

$$\mathbf{G}=\sum_{i=1}^{n} \mathbf{G}_i \tag{18}$$

holds for the components parallel to the surface plane. If (18) is not satisfied perpendicular to this plane, the prefactor of the associated exponential of the OP's is small, when the mismatch of the $\mathbf{G}$'s is small. Equation (17) shows that higher-order corrections do not affect the maximum of the $a_{\mathbf{G}}$'s but may modify the other $a_{\mathbf{G}}$'s. However, $a((10))$, $a((01))$, and $a((00))$ (in the notation of Figs. 3 and 4) are not altered by higher-order corrections.

For a long-ranged r^{-n} potential (e.g., $n=6$), which we assume to be slowly varying, i.e., whose Fourier transform vanishes beyond the first Brillouin zone of the solid lattice, we find[4] that $\rho_{(000)}(z)$ approaches zero as a power law $\sim z^{-(n-3)}$. This implies $a_{(000)}\to\infty$. The decay of the other OP's remains unaffected. This modifies the temperature dependence of the residual crystallinity[4] into a stretched exponential $\sim\exp(A_{\mathbf{G}}t^{-1/3})$ with $A_{\mathbf{G}}=(2W)^{1/3}/a_{\mathbf{G}}$, where W denotes the Hamaker constant.

VI. CONCLUSIONS

In conclusion, we have presented a microscopic expression, based on the Fourier transform of the direct correlation function, for the characteristic lengths governing the decay of the Fourier coefficients of the solid density within the liquid. For a hard sphere plus Lennard-Jones potential, we calculate these decay lengths using the ORPA. We have also discussed the dependence of the decay length on the orientation of the surface plane and the influence of oscillatory potentials. The latter may enhance or reduce the crystallinity in a quasi-liquid film considerably if the inverse oscillation length (i.e., the Fermi momentum for a metal) is comparable to the first RLV of the solid. For Pb and Al, we used data of the liquid structure factor in order to determine the decay lengths. The results are in accordance with LEED experiments. Further experiments (e.g., by using totally reflected x rays) are highly desirable in order to obtain a more detailed comparison with the theory.

ACKNOWLEDGMENTS

We thank H. Wagner, R. Lipowsky, S. Dietrich, and D. Kroll for useful discussions.

[1]K. C. Prince, U. Breuer, and H. P. Bonzel, Phys. Rev. Lett. **60**, 1146 (1988).

[2]U. Breuer, H. P. Bonzel, K. C. Prince, and R. Lipowsky, Surf. Sci. **223**, 258 (1989).

[3]R. Lipowsky, U. Breuer, K. C. Prince, and H. P. Bonzel, Phys. Rev. Lett. **62**, 913 (1989).

[4]H. Löwen, T. Beier, H. Wagner, Europhys. Lett. **9**, 791 (1989); Z. Phys. B (to be published).

[5]L. V. Mikheev and A. A. Chernov, Zh. Eskp. Teor. Fiz. **92**, 1732 (1987) [Sov. Phys.—JETP **65**, 971 (1987)].

[6]W. H. Shih, Z. Q. Wang, X. C. Zheng, and D. Stroud, Phys. Rev. A **35**, 2611 (1987); G. Gompper and D. Kroll, Phys. Rev. B **40**, 7221 (1989).

[7]S. M. Foiles and N. W. Ashcroft, J. Chem. Phys. **75**, 3594 (1981).

[8]J. P. Hansen and I. R. McDonald, *Theory of Simple Liquids* (Academic, New York, 1976); J. A. Barker and D. Henderson, Rev. Mod. Phys. **48**, 587 (1976).

[9]N. E. Cusack, *The Physics of Structurally Disordered Matter, Graduate Student Series in Physics* (Hilger, London, 1987).

[10]L. Verlet and J. J. Weis, Phys. Rev. A **5**, 939 (1972); D. Henderson and E. W. Grundke, J. Chem. Phys. **63**, 601 (1975).

[11]A. Trayanov and E. Tosatti, Phys. Rev. Lett. **59**, 2207 (1987); Phys. Rev. B **38**, 6961 (1988).

[12]See, e.g., D. G. Pettifor and M. A. Ward, Solid State Commun. **49**, 291 (1984).

[13]For an application of the ORPA to liquid metals see, e.g., G. Kahl and J. Hafner, Phys. Rev. A **29**, 3310 (1984); Z. Phys. B

58, 283 (1985).
[14]J. P. Hansen and L. Verlet, Phys. Rev. **184**, 151 (1969).
[15]Y. Waseda, *The Structure of Non-Crystalline Materials* (McGraw-Hill, New York, 1980).
[16]H. Löwen (unpublished).
[17]B. Pluis, T. N. Taylor, D. Frenkel, and J. F. van der Veen, Phys. Rev. B **40**, 1353 (1989); see also J. Frenken, P. M. Maree, and J. F. van der Veen, *ibid.* **34**, 7506 (1986).